



Intercomparison of two cavity ring-down spectroscopy analyzers for atmospheric $^{13}\text{CO}_2$ / $^{12}\text{CO}_2$ measurement

Jiaping Pang^{1,2}, Xuefa Wen^{1,2}, Xiaomin Sun^{1,2}, and Kuan Huang³

¹Key Laboratory of Ecosystem Network Observation and Modeling, Institute of Geographic Sciences and Natural Resources Research, Chinese Academy of Sciences, Beijing 100101, China

²University of Chinese Academy of Sciences, Beijing 100049, China

³Picarro, Inc., Santa Clara, California 95054, USA

Correspondence to: Xuefa Wen (wenxf@igsnr.ac.cn) and Xiaomin Sun (sunxm@igsnr.ac.cn)

Received: 22 March 2016 – Published in Atmos. Meas. Tech. Discuss.: 25 April 2016

Revised: 28 July 2016 – Accepted: 31 July 2016 – Published: 22 August 2016

Abstract. Isotope ratio infrared spectroscopy (IRIS) permits continuous in situ measurement of CO_2 isotopic composition under ambient conditions. Previous studies have mainly focused on single IRIS instrument performance; few studies have considered the comparability among different IRIS instruments. In this study, we carried out laboratory and ambient measurements using two Picarro $\text{CO}_2\delta^{13}\text{C}$ analyzers (G1101-i and G2201-i (newer version)) and evaluated their performance and comparability. The best precision was 0.08–0.15 ‰ for G1101-i and 0.01–0.04 ‰ for G2201-i. The dependence of $\delta^{13}\text{C}$ on CO_2 concentration was 0.46 ‰ per 100 ppm and 0.09 ‰ per 100 ppm, the instrument drift ranged from 0.92–1.09 ‰ and 0.19–0.37 ‰, and the sensitivity of $\delta^{13}\text{C}$ to the water vapor mixing ratio was 1.01 ‰ / % H_2O and 0.09 ‰ / % H_2O for G1101-i and G2201-i, respectively. The accuracy after correction by the two-point mixing ratio gain and offset calibration method ranged from –0.04–0.09 ‰ for G1101-i and –0.13–0.03 ‰ for G2201-i. The sensitivity of $\delta^{13}\text{C}$ to the water vapor mixing ratio improved from 1.01 ‰ / % H_2O before the upgrade of G1101-i (G1101-i-original) to 0.15 ‰ / % H_2O after the upgrade of G1101-i (G1101-i-upgraded). Atmospheric $\delta^{13}\text{C}$ measured by G1101-i and G2201-i captured the rapid changes in atmospheric $\delta^{13}\text{C}$ signals on hourly to diurnal cycle scales, with a difference of 0.07 ± 0.24 ‰ between G1101-i-original and G2201-i and 0.05 ± 0.30 ‰ between G1101-i-upgraded and G2201-i. A significant linear correlation was observed between the $\delta^{13}\text{C}$ difference of G1101-i-original and G2201-i and the water vapor concentration, but there was no significant correlation between the $\delta^{13}\text{C}$ differ-

ence of G1101-i-upgraded and G2201-i and the water vapor concentration. The difference in the Keeling intercept values decreased from 1.24 ‰ between G1101-i-original and G2201-i to 0.36 ‰ between G1101-i-upgraded and G2201-i, which indicates the importance of consistency among different IRIS instruments.

1 Introduction

The development of stable isotope analyzers and measurement techniques has made stable isotope analysis a powerful tool for gaining insight into the underlying mechanisms of carbon and water cycling in atmospheric, ecological, and hydrological studies (Yakir and Sternberg, 2000; Bowling et al., 2003; Griffis, 2013). Isotope ratio infrared spectroscopy (IRIS) permits in situ and continuous isotope measurements under ambient conditions and overcomes the shortcoming of traditional isotope ratio mass spectrometers (IRMS), which involve relatively labor-intensive sample collection and preparation (Bowling et al., 2005; Schaeffer et al., 2008; Wingate et al., 2010; Griffith et al., 2012; Werner et al., 2012; Griffis, 2013). To date, various IRIS techniques are commercially available for measuring stable carbon isotopes, including lead-salt tunable diode laser absorption spectrometry (TDLAS, Campbell Scientific Inc.), wavelength-scanned cavity ring-down spectroscopy (WS-CRDS, Picarro Inc.), off-axis cavity output spectroscopy (OA-ICOS, Los Gatos Research), quantum cascade laser absorption spectrometry (QCLAS, Aerodyne Research), and difference fre-

quency generation laser spectroscopy (DFG, Thermo Scientific; Griffiths, 2013; Wen et al., 2012, 2013). All the data monitored by IRIS analyzers should capture the $\delta^{13}\text{C}$ variations of atmospheric CO_2 with high precision under ambient conditions and should be traceable to the standard Vienna Pee Dee Belemnite (VPDB) scale (Bowling et al., 2005; Schaeffer et al., 2008; Griffiths, 2013). To assess the data comparability of different experiments, it is important to conduct an intercomparison of different IRIS instruments to ensure their compatibility (Flowers et al., 2012; Griffiths et al., 2012; Wen et al., 2013).

Previous studies have shown that temperature dependence, concentration dependence, and spectroscopic interference are among the major sources of errors for IRIS measurements (Griffiths et al., 2012; Guillon et al., 2012; Vogel et al., 2013; Wen et al., 2013). Instrument long-term drift is another source of errors affecting IRIS performance (Rella et al., 2013; Vogel et al., 2013). Most previous studies focus on the methodology of a single IRIS instrument (Bowling et al., 2003; Wahl et al., 2006; Tuzson et al., 2008; Griffiths et al., 2012; Guillon et al., 2012; Vogel et al., 2013). It is important to obtain precise and accurate measurements that are traceable to the international VPDB standard by improving measurement precision and by constructing a proper calibration strategy. Previous laboratory and field experiments showed precision of IRIS instruments ranging from 0.02 to 0.25‰ for $\delta^{13}\text{C}$ (Bowling et al., 2003; Wahl et al., 2006; Schaeffer et al., 2008; Tuzson et al., 2008; Griffiths et al., 2012; Guillon et al., 2012; Sturm et al., 2012; Vogel et al., 2013; Wen et al., 2013). Because of the nonlinear response of the concentration dependence of IRIS instruments, it is recommended that more than two standard gases with different CO_2 concentrations be used for the $^{12}\text{CO}_2$ and $^{13}\text{CO}_2$ calibration to eliminate the nonlinear response of the instruments (Bowling et al., 2005; Schaeffer et al., 2008; Tuzson et al., 2008). The accuracy of $\delta^{13}\text{C}$ is $0.01 \pm 0.03\%$ for the three-point linear calibration and $0.00 \pm 0.01\%$ for the four-point linear calibration (Bowling et al., 2005). Setting the proper calibration frequency according to the stability of the instrument can eliminate the drift and the environmental sensitivity of the instruments (Griffiths, 2013; Wen et al., 2013).

System bias among different IRIS instrument measurements would result in poor measurement comparability (Flowers et al., 2012; Hammer et al., 2013; Griffiths, 2013; Wen et al., 2013). Bowling et al. (2003) found a consistent $\delta^{13}\text{C}$ offset of $1.77 \pm 0.35\%$ between the TDLAS and flask-IRMS measurement ($n = 82$) that was caused by pressure broadening. Schaeffer et al. (2008) compared the TDLAS and portable flask package sampling-IRMS measurement and observed a difference of $0.01 \pm 0.45\%$ ($n = 277$) for $\delta^{13}\text{C}$. Tuzson et al. (2008) found a difference between QCLAS and flask-IRMS measurement of 0.28–2‰ that was probably caused by nonlinearity of the QCL instrument at elevated CO_2 concentrations and laser intensity variation. Note that an ideal IRIS instrument should be free of nonlinear ab-

sorption or concentration dependence effects, meaning that its measurements should not change with the changing CO_2 concentrations at a constant isotopic composition. Mohn et al. (2008) observed a mean difference of 0.4‰ ($n = 81$) between Fourier transform infrared spectroscopy (FTIR) and flask-IRMS measurements. Considering the time resolution difference between IRIS and IRMS sampling technology, a clear difference was observed when rapid changes in the atmospheric CO_2 concentration occurred (Schaeffer et al., 2008). Mohn et al. (2008) used the Keeling plot method to eliminate the difference in the sampling time resolution between IRMS and FTIR. The difference of $\delta^{13}\text{C}_R$ obtained by this method was insignificant (-28.1 ± 0.4 and $-27.9 \pm 0.5\%$). Very few studies have compared IRIS instruments (Griffiths, 2013; Wen et al., 2013); only Wen et al. (2013) compared two commercially available IRIS instruments, Los Gatos DLT-100 and Picarro G1101-i, which had excellent agreement over a 7-day atmospheric measurement period, with a difference of only $-0.02 \pm 0.18\%$ after proper calibration. However, there was still a slight correlation of the difference between the two analyzers with concentration. This slight concentration dependence resulted in a much larger difference (2.44‰) for the Keeling intercept by propagating through the Keeling analysis.

The objective of this study is to evaluate the performance and comparability of two Picarro $\text{CO}_2\delta^{13}\text{C}$ analyzers based on CRDS technology (G1101-i and G2201-i). We aim to (1) determine the optimal precision of both analyzers by Allan deviation; (2) test the dependence of $\delta^{13}\text{C}$ on CO_2 concentration, drift, and accuracy using a gradient switching experiment; (3) identify the sensitivity of $\delta^{13}\text{C}$ to the water vapor mixing ratio using a dew point generator; and (4) examine the compatibility of G1101-i and G2201-i using atmospheric $\text{CO}_2\delta^{13}\text{C}$ measurements. The laboratory and atmospheric measurements data are available at https://www.researchgate.net/publication/301644542_Inter-comparison_of_two_cavity_ring-down_spectroscopy_analyzers_for_atmospheric_13CO2_12CO2_measurement.

2 Materials and methods

2.1 Analyzers, sampling, and calibration systems

In this study, the inlets of two $\text{CO}_2\delta^{13}\text{C}$ analyzers of Picarro Inc., Sunnyvale, CA, G1101-i (manufactured in 2010) and G2201-i (manufactured in 2014), were connected in parallel and then connected with three three-way solenoid valves, which constitutes the sampling and calibration system with one ambient air inlet and three calibration gas inlets (Fig. 1). The switch sequence of valves was controlled by the valve sequencer software on the G2201-i analyzer. The built-in pressure and temperature monitoring systems of G1101-i and G2201-i maintained the cavity temperature of both systems at 45 °C and the cavity pressures at 140

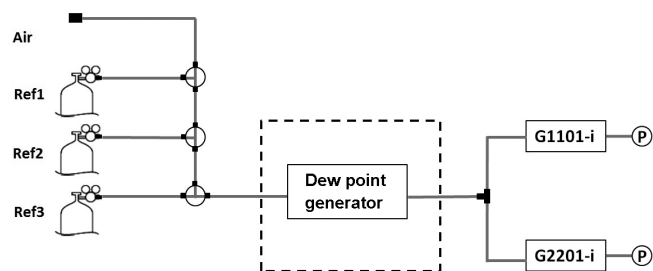


Figure 1. Schematic setup of the laboratory and ambient measurements of two Picarro $\text{CO}_2 \delta^{13}\text{C}$ analyzers.

and 148 Torr, respectively. The observed stability of temperature over 24 h was 45.0 ± 0.0024 and 45.0 ± 0.0005 °C, and the observed stability of pressure was 140.0429 ± 0.0580 and 147.9990 ± 0.0165 Torr for G1101-i and G2201-i, respectively. No relationship between temperature and pressure variation and the $\delta^{13}\text{C}$ difference of either instrument was found. A diaphragm pump was used to pump the sample air and calibration gas continuously to the cavity (volume of 35 mL) at a flow rate of 0.03 L min^{-1} at standard temperature and pressure (STP); measurement frequencies were approximately 0.3 and 1 Hz for G1101-i and G2201-i, respectively. Note that the turnover time of sample air in the analyzer is not fast enough for 0.3 and 1 Hz data to be meaningful. In this study, the data reported were block-averaged to average time intervals after deleting the data collected during transitional periods in response to valve switching between the two sample intakes. The physical laser arrays and the software of the G1101-i analyzer were upgraded in March 2012 and August 2014 to correct the cross-interference caused by CH_4 and water vapor, respectively. In the following laboratory and atmospheric measurements, the water vapor sensitivity test and atmospheric measurements were done before the upgrade of G1101-i (G1101-i-original) and after the upgrade of G1101-i (G1101-i-upgraded) in August 2014.

The sample air stream passed through a filter (pore size 2 μm , Swagelok model B-4F-05, Connecticut Valves and Fittings, Norwalk Connecticut) to the analyzers without being dried. In this study, only the water vapor dilution effect was corrected, without considering the water vapor pressure broadening effect and the spectral interference effect (Wen et al., 2013). Data from the transitional periods, i.e., the first 180 s of each sample measurement cycle after valve switching, were discarded. The transitional periods in response to valve switching between two air sample intakes were about 120 s.

2.2 Laboratory measurement

Three reference gases (Ref1, Ref2, and Ref3) were produced by Beijing AP BAIF Gases Industry Co., Ltd, with CO_2 mixing ratios of 368.1, 451.7, and 550.1 ppm. The $\delta^{13}\text{C}$ values were measured using an isotope ratio mass spectrom-

eter (Thermo Finnigan MAT 253) at the Key Laboratory of Ecosystem Network Observation and Modeling, Institute of Geographic Sciences and Natural Resources Research, Chinese Academy of Sciences. Because the three reference gases originated from the same gas source, the $\delta^{13}\text{C}$ values were -20.38 ± 0.06 ‰ for all three reference gases.

2.2.1 Allan variance test

Allan variance (Allan, 1987; Werle et al., 1993) is commonly used to express measurement precision and stability as a function of average time. Here Ref1, Ref2, and Ref3 were connected to the sampling and calibration systems and were each measured for 24 h to conduct the Allan variance analysis for G1101-i-original and G2201-i.

2.2.2 Gradient switching test

Ref1, Ref2, and Ref3 were connected to the sampling and calibration system and switched sequentially every 40 min for a total of 48 h. Two of the three reference gases were treated as calibration gases and the third was treated as the target gas. The two-point mixing ratio gain and offset calibration strategy (Bowling et al., 2003; Wen et al., 2013) was used for each 120 min measurement cycle. The measured data and calibrated data were used to evaluate the dependence of $\delta^{13}\text{C}$ on CO_2 concentration, and long-term drift as well as the accuracy of both the G1101-i-original and G2201-i analyzers.

2.2.3 Water vapor sensitivity test

The water vapor sensitivity of both analyzers was tested by connecting the reference gas (Ref1) to a dew point generator (model LI-610, Li-Cor, Inc., Lincoln, NE, USA). The reference gas (Ref1) bubbled through the reservoir of the dew point generator to produce different humidity levels by setting different dew point temperatures. The dissolution of CO_2 in the reservoir (25–30 mL) of the dew point generator moved quickly into a dynamic equilibrium state because of the carbonate chemistry in solution at different dew point temperatures, which did not change the true $\delta^{13}\text{C}$ signal because of lasting bubbled processes. The first test was conducted in June 2014 for both G1101-i-original and G2201-i analyzers; the dew point temperatures were 5.0, 10.0, 15.0, 20.0, and 25.0 °C, and the corresponding water vapor ranged from 0.87 to 3.15 %. The second test was conducted in December 2014 for the G1101-i-upgraded and G2201-i analyzers; the dew point temperatures were 1.0, 5.0, 10.0, 15.0, and 20.0 °C, and the corresponding water vapor ranged from 0.65 to 2.32 %. Reference gas at each humidity level was measured for 20 min a total of three times.

2.3 Atmospheric measurement

The air sample inlet was located outside the Key Laboratory of Ecosystem Network Observation and Modeling, 10 m above the ground (Wen et al., 2008, 2010, 2012, 2013). The first atmospheric measurement dataset was collected, for both the G1101-i-original and G2201-i analyzers, from 15 June 2015 to 23 June 2015 (DOY 164–174), and the second dataset was collected, for both G1101-i-upgraded and G2201-i analyzers, from 14 December to 22 December 2014 (DOY 348–356). The first atmospheric measurement sampled Ref1 and Ref3 for 10 min each, followed by alternate measurements of ambient air (50 min) and Ref2 (10 min) for 5 h. The total duration of the sampling and calibration cycle was 320 min. The second atmospheric measurement sampled Ref1, Ref2, and Ref3 for 10 min each, followed by ambient air measurement for 300 min, i.e., a total duration of 330 min for each sampling and calibration cycle. The atmospheric sample and Ref2 were calibrated by Ref1 and Ref3 for each measurement cycle, and the calibrated atmospheric sample data were used to obtain hourly mean values.

2.4 Calibration procedures

The two-point mixing ratio gain and offset calibration method (Bowling et al., 2003) was used to calibrate the $^{12}\text{CO}_2$ and $^{13}\text{CO}_2$ mixing ratio measured by G1101-i and G2201-i. Additional details about the calibration method can be found in Wen et al. (2013). Following this method, the calibrated mixing ratios of $^{12}\text{CO}_2$ (x^{12}) and $^{13}\text{CO}_2$ (x^{13}) are calculated as

$$x_{a,t}^{12} = \frac{x_{3,t}^{12} - x_{1,t}^{12}}{x_{3,m}^{12} - x_{1,m}^{12}} (x_{a,m}^{12} - x_{1,m}^{12}) + x_{1,t}^{12} \quad (1)$$

$$x_{a,t}^{13} = \frac{x_{3,t}^{13} - x_{1,t}^{13}}{x_{3,m}^{13} - x_{1,m}^{13}} (x_{a,m}^{13} - x_{1,m}^{13}) + x_{1,t}^{13} \quad (2)$$

where m and t represent the measured and true mixing ratios, and the subscripts 1, 3, and a represent Ref1, Ref3, and ambient air, respectively.

The isotopic composition of CO_2 in the ambient air is expressed in the delta notation:

$$\delta^{13}\text{C} = (R_{\text{sample}}/R_{\text{VPDB}} - 1) \times 1000, \quad (3)$$

where R_{sample} is the $^{13}\text{C}/^{12}\text{C}$ ratio of the sample, and R_{VPDB} is the $^{13}\text{C}/^{12}\text{C}$ ratio of the reference standard (i.e., the VPDB).

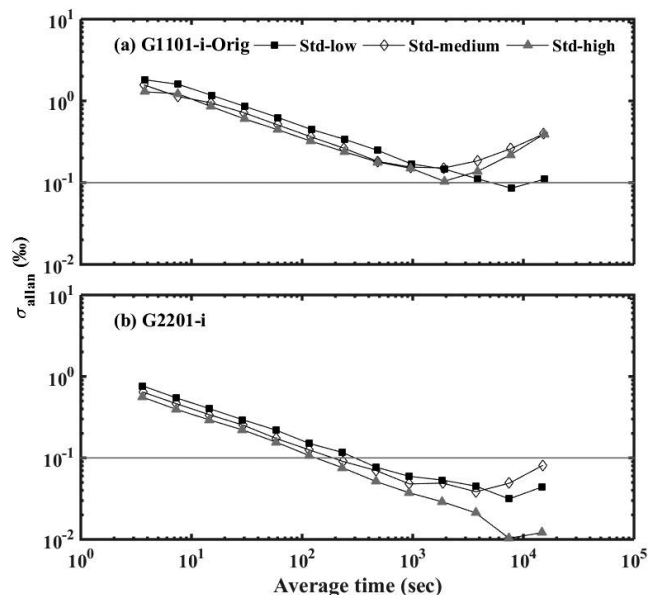


Figure 2. Allan deviation of the $\delta^{13}\text{C}$ at endpoint for the (a) G1101-i before upgradation (G1101-i-original) and (b) G2201-i analyzers with three different CO_2 concentrations with same $\delta^{13}\text{C}$ standard gases.

3 Results

3.1 Precision

Figure 2 shows the Allan variance (Allan, 1987) as a function of the average time of the $\delta^{13}\text{C}$ measurements for Ref1, Ref2, and Ref3 measured by G1101-i-original and G2201-i. If the Allan variance is dominated by the random white (Gaussian) noise, the Allan variance should decrease linearly with average time, and the precision should increase with the average time. However, for longer average times, the precision worsens because of instrumental drift. In addition, the precision should increase with increasing CO_2 concentrations because of high signal-to-noise ratio. The $\delta^{13}\text{C}$ precision improved with the average time and achieved optimum values of 0.08, 0.15, and 0.10 ‰ for G1101-i-original at 7600, 1900, and 1900 s for Ref1, Ref2 and Ref3, respectively and 0.03, 0.04, and 0.01 ‰ for G2201-i at 7600, 3800, and 7600 s for the three reference gases, respectively. The 5 min precision was 0.24–0.34 ‰ and 0.08–0.12 ‰ for G1101-i-original and G2201-i, respectively (Table 1).

The precisions of G1101-i-original and G2201-i $\delta^{13}\text{C}$ values were comparable with other reported performances of IRIS instruments. The precision of TDLAS instruments ranged from 0.03 to 4 ‰ (Bowling et al., 2003, 2005; Griffis et al., 2004; Pataki et al., 2006). Picarro EnviroSense 2050 had a precision of 0.08 ‰ at 130 min (Friedrichs et al., 2010). The Picarro G1101-i had a precision of 0.2 ‰ at 5 min (Vogel et al., 2013), and the best precision of 0.08 ‰

Table 1. Measurement precision (Allan deviation for 1 min, 5 min and optimum averaging times) from three reference gases (Ref1, Ref2 and Ref3) with 0.3 and 1 Hz sampling rate for the Picarro G1101-i before upgradation (G1101-i-original) and G2201-i analyzers.

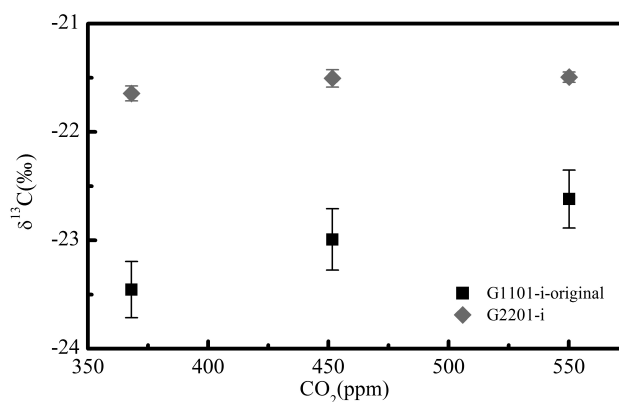
Species		Averaging time					
		G2201-i			G1101-i-original		
		1 min	5 min	Optimum	1 min	5 min	Optimum
$^{12}\text{CO}_2$	Ref1	0.03	0.02	0.01	0.07	0.03	0.01
	Ref2	0.04	0.02	0.01	0.07	0.04	0.02
	Ref3	0.04	0.02	0.01	0.08	0.04	0.01
	Mean	0.04	0.02	0.01	0.07	0.04	0.02
$^{13}\text{CO}_2$	Ref1	0.0009	0.0005	0.0001	0.0025	0.0014	0.0006
	Ref2	0.0009	0.0004	0.0003	0.0025	0.0013	0.0008
	Ref3	0.0009	0.0004	0.0001	0.0032	0.0016	0.0007
	Mean	0.0009	0.0004	0.0002	0.0027	0.0014	0.0007
$\delta^{13}\text{C}$	Ref1	0.22	0.12	0.03	0.63	0.34	0.08
	Ref2	0.17	0.09	0.04	0.51	0.26	0.15
	Ref3	0.16	0.08	0.01	0.44	0.24	0.10
	Mean	0.18	0.09	0.03	0.53	0.28	0.13

at 2000 s (Wen et al., 2013). For Los Gatos DLT-100, the optimal precision of 0.04‰ was obtained at 1000 s (Wen et al., 2013). The QCLAS typically has a precision of 0.18‰ at 350 ppm CO_2 (McManus et al., 2005), and the optimal precision of 0.16‰ was obtained at 500 s (Tuzson et al., 2008). Nicolet Avatar 370 (Thermo Electron, USA) based on FTIR technology obtained the optimal precision of 0.15‰ at 16 min (Mohn et al., 2007), and an improved version had a precision of 0.02‰ at 10 min (Griffith et al., 2012).

3.2 Concentration dependence

Figure 3 shows the dependence of $\delta^{13}\text{C}$ on CO_2 concentration for G1101-i-original and G2201-i. The dependence of $\delta^{13}\text{C}$ on CO_2 concentration is the nonlinearity of the analyzer response to CO_2 concentration variance (Griffith et al., 2012; Guillon et al., 2012; Wen et al., 2013). The $\delta^{13}\text{C}$ values of Ref1, Ref2, and Ref3 measured by G1101-i-original were -23.46 ± 0.26 , -22.99 ± 0.28 , and -22.62 ± 0.27 ‰, with an average value of -23.02 ± 0.27 ‰. The $\delta^{13}\text{C}$ values measured by G2201-i were -21.65 ± 0.07 , -21.51 ± 0.08 , and -21.49 ± 0.05 ‰, with an average value of -21.55 ± 0.07 ‰ (Fig. 3). In the range of 368.1–550.1 ppm, $\delta^{13}\text{C}$ values measured by G1101-i-original and G2201-i showed an increase with an increase of CO_2 concentration at 0.46‰ per 100 ppm and 0.09‰ per 100 ppm, respectively, and the peak-to-peak amplitudes were 1.75 and 0.47‰, respectively.

The concentration dependence of the measured $\delta^{13}\text{C}$ values is the main error source affecting IRIS measurements. Guillon et al. (2012) found that the DLT-100 based on ICOS technology had a nonlinear concentration dependence in the range 300–2000 ppm. After correcting the concentration de-

**Figure 3.** Dependency of the measured $\delta^{13}\text{C}$ of G1101-i before upgradation (G1101-i-original) and G2201-i analyzers on the measured CO_2 concentration with three different CO_2 concentrations with same $\delta^{13}\text{C}$ reference gases.

pendence by a fifth-order polynomial calibration curve, the accuracy improved from 2.7 to 1.3‰ for $\delta^{13}\text{C}$. The Picarro G1101-i analyzer, based on CRDS technology, showed no significant concentration dependence of $\delta^{13}\text{C}$ with a standard deviation of ~ 0.2 ‰ in the range 303–437 ppm (Vogel et al., 2013). Griffith et al. (2012) used a series of different CO_2 mixing ratios at constant $\delta^{13}\text{C}$, and found that a residual curvature against the reciprocal of CO_2 was caused by a small nonlinear response of the analyzer.

3.3 Stability and accuracy

Based on the same data measured in Sect. 3.2, the temporal drift and accuracy of $\delta^{13}\text{C}$ values of Ref1, Ref2,

Table 2. The stability and accuracy of $\delta^{13}\text{C}$ values of the three reference gases (Ref1, Ref2, and Ref3) with same $\delta^{13}\text{C}$ measured by G1101-i before upgradation (G1101-i-original) and G2201-i analyzers.

	G1101-i-original		G2201-i		IRMS
	Measured	Corrected	Measured	Corrected	
Ref1	-23.46 ± 0.26	-20.29 ± 0.34	-21.65 ± 0.07	-20.51 ± 0.21	-20.38 ± 0.06
Ref2	-22.99 ± 0.28	-20.42 ± 0.20	-21.51 ± 0.08	-20.35 ± 0.08	-20.38 ± 0.06
Ref3	-22.62 ± 0.27	-20.32 ± 0.21	-21.49 ± 0.05	-20.48 ± 0.14	-20.38 ± 0.06

and Ref3 measured by G1101-i-original and G2201-i are shown in Fig. 4. The two-point mixing ratio gain and offset calibration method (Bowling et al., 2003) was used to calibrate the measured $\delta^{13}\text{C}$ value for each 120 min measurement cycle. The instrument temporal drift was calculated as the maximum variability during the measurement period, which mainly resulted from the sensitivity to the changing environmental conditions (e.g., temperature dependence). During the 48 h measuring period, the standard deviations of $\delta^{13}\text{C}$ values of Ref1, Ref2, and Ref3 measured by G1101-i-original were 0.26, 0.28, and 0.27 ‰, respectively, with temporal drifts (peak-to-peak magnitude) of 0.92, 1.09, and 0.93 ‰. The standard deviations of the $\delta^{13}\text{C}$ values of Ref1, Ref2, and Ref3 measured by G2201-i were 0.07, 0.08, and 0.05 ‰, with temporal drifts of 0.23, 0.37, and 0.19 ‰. The differences between the CRDS and IRMS measurements were -3.08 ± 0.26 , -2.61 ± 0.28 , and -2.24 ± 0.27 ‰ for G1101-i-original and -1.27 ± 0.07 , -1.13 ± 0.08 , and -1.11 ± 0.05 ‰ for G2201-i. After calibration, the differences reduced to 0.09 ± 0.34 , 0.04 ± 0.20 , and 0.06 ± 0.21 ‰ for G1101-i and -0.13 ± 0.21 , 0.03 ± 0.08 , and -0.10 ± 0.14 ‰ for G2201-i (Table 2). Much improved accuracy was obtained when the calibration was interpolated for Ref2 with Ref1 and Ref3 rather than extrapolated for Ref1 with Ref2 and Ref3 or Ref3 with Ref1 and Ref2.

As for the drift of IRIS instruments, Vogel et al. (2013) monitored two gas cylinders sequentially with 10 min and 20 min for each cylinder lasting 3 days; the drift of G1101-i was around 0.3 ‰ day^{-1} . Hammer et al. (2013) measured a target gas continuously for 6 days; the FTIR instrument showed a drift of 0.02 ‰ day^{-1} for $\delta^{13}\text{C}$ after sensitivity correction. Tuzson et al. (2008) measured identical air samples for 1 min every 15 min for 7 h; the standard deviation of the $\delta^{13}\text{C}$ measured by QCLAS was 0.14 ‰ ($n = 28$). Schaeffer et al. (2008) monitored two quality control tanks in the field over 2.44 years, and the standard deviations of the difference between actual and measured values were 0.31 and 0.33 ‰ ($n = 2318$ and $n = 2254$). Wehr et al. (2008) monitored a CSIRO standard gas over a period of 30 min, and the standard deviations for integration times of 20 and 120 s were 0.71 and 0.64 ‰, respectively. In this study, over a period of 48 h, the standard deviations of $\delta^{13}\text{C}$ measured by G1101-i-original and G2201-i were 0.26–0.28 and 0.05–0.08 ‰, re-

spectively, and the drift values were 0.92–1.09 and 0.19–0.37 ‰, respectively.

Regarding the accuracy of IRIS instruments, Guillon et al. (2012) found that in the range 300–2000 ppm, the accuracy of $\delta^{13}\text{C}$ measured by DLT-100 was 2.7 ‰ for raw measurements and improved to 1.3 ‰ after correction. Over the entire 2.44-year period, two quality control gases measured by TDLAS in the field showed agreement between actual and measured values of -0.17 ± 0.33 and -0.14 ± 0.4 ‰ for tank 1 and tank 2 (Schaeffer et al., 2008). Over a period of 30 min, the $\delta^{13}\text{C}$ values measured by optical feedback cavity enhanced absorption spectroscopy (OF-CEAS) showed a systematic error of 0.9 ‰ between the measured and IRMS values (Wehr et al., 2008). Using the optimized PLS algorithm, the accuracy of $\delta^{13}\text{C}$ measured by FTIR was 0.4 ‰ with CO_2 concentrations in the range 364–530 ppm (Mohn et al., 2007). Over a 1-year period, Vogel et al. (2013) found that although a single measurement was imprecise, the G1101-i $\delta^{13}\text{C}$ analyzer provided a mean accuracy of 0.002 ± 0.025 ‰ after proper calibration. In this study, the accuracies of G1101-i-original and G2201-i $\delta^{13}\text{C}$ analyzers were -3.06 to -2.22 and -1.25 to -1.09 ‰ before calibration and improved to -0.02 – 0.11 and -0.11 – 0.05 ‰ after calibration for each 120 min measurement cycle over a measurement course of 48 h.

3.4 Sensitivity of $\delta^{13}\text{C}$ to water vapor concentration

The sensitivities of $\delta^{13}\text{C}$ to water vapor concentration of G1101-i-original and G2201-i before the upgrade of G1101-i and G1101-i-upgraded and G2201-i after the upgrade of G1101-i are shown in Fig. 5. For the first test, the dew point temperature of the reference gas ranged from 5 to 25 °C. The mean $\delta^{13}\text{C}$ values measured by G1101-i-original and G2201-i were -20.64 ± 0.72 and -21.60 ± 0.19 ‰, the sensitivity of $\delta^{13}\text{C}$ to the water vapor mixing ratio was 0.86 ‰ / % H_2O and 0.20 ‰ / % H_2O , and the peak-to-peak amplitudes of $\delta^{13}\text{C}$ under different water vapor mixing ratios were 1.96 and 0.45 ‰, respectively. For the second test, the mean $\delta^{13}\text{C}$ values measured by G1101-i-upgraded and G2201-i were -22.34 ± 0.09 and -22.27 ± 0.18 ‰, the sensitivity of $\delta^{13}\text{C}$ to the water vapor mixing ratio was 0.13 ‰ / % H_2O and -0.19 ‰ / % H_2O , and the peak-to-peak amplitudes of $\delta^{13}\text{C}$ under different water vapor mixing ratios were

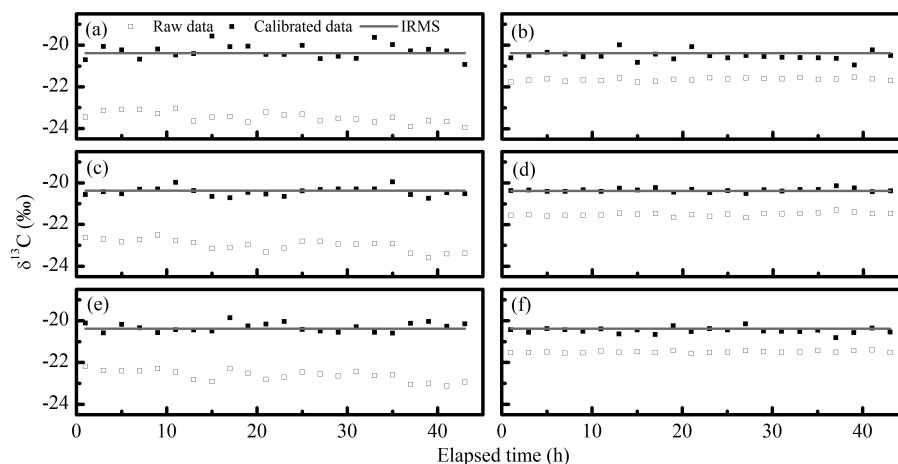


Figure 4. Time variations of $\delta^{13}\text{C}$ of the three different CO_2 concentrations with same $\delta^{13}\text{C}$ reference gases (Ref1, Ref2 and Ref3) of G1101-i before upgradation (G1101-i-original) (a, c, e) and G2201-i (b, d, f) analyzers. Panels (a) and (b) show data from Ref1, panels (c) and (d) show data from Ref2, and panels (e) and (f) show data from Ref3.

0.22 and 0.32‰, respectively. Note that with the dew point in the range of 5–20 °C, the mean $\delta^{13}\text{C}$ values measured were -20.84 ± 0.66 and -21.68 ± 0.07 ‰ by G1101-i-original and G2201-i, respectively, and -22.34 ± 0.10 and -22.34 ± 0.08 ‰ by G1101-i-upgraded and G2201-i, respectively. The sensitivity of $\delta^{13}\text{C}$ to the water vapor mixing ratio was 1.01‰/% H_2O and 0.09‰/% H_2O , and the peak-to-peak amplitudes were 1.47 and 0.14‰ by G1101-i-original and G2201-i, respectively. The sensitivity of $\delta^{13}\text{C}$ to the water vapor mixing ratio was 0.15‰/% H_2O and 0.13‰/% H_2O , and the peak-to-peak amplitudes were 0.22 and 0.19‰ for G1101-i-upgraded and G2201-i, respectively.

The dilution and pressure broadening effects are the two major factors leading to the dependence of the measured $\delta^{13}\text{C}$ on water vapor concentrations (Chen et al., 2010; Nara et al., 2012). Variations in sample water vapor significantly affect the mixing ratio of $^{12}\text{CO}_2$ and $^{13}\text{CO}_2$ via the dilution effect. In addition, the variability of water vapor also introduces the broadening effect along the spectroscopic line, which includes the Lorentzian line broadening and Dicke line narrowing effect. The CRDS instruments measured $^{12}\text{CO}_2$ and $^{13}\text{CO}_2$ concentrations by the peak height of the absorption peak whose baseline and shape can be affected by the absorption peaks of water (Nara et al., 2012; Rella et al., 2013). As for CO_2 , the systematic errors caused by the broadening effects would be 40% of the dilution effects if they were not corrected (Chen et al., 2010). The transferability of water correction functions among multiple instruments also biases the measurement data among different instruments. Rella et al. (2013) found that for analyzers CFADS15 and 30, the transferability of both CO_2 and CH_4 , after correction of the water vapor mole fraction in the range no more than 2%, meets the Global Atmosphere Watch (GAW) Programme quality. For three instruments based on CRDS tech-

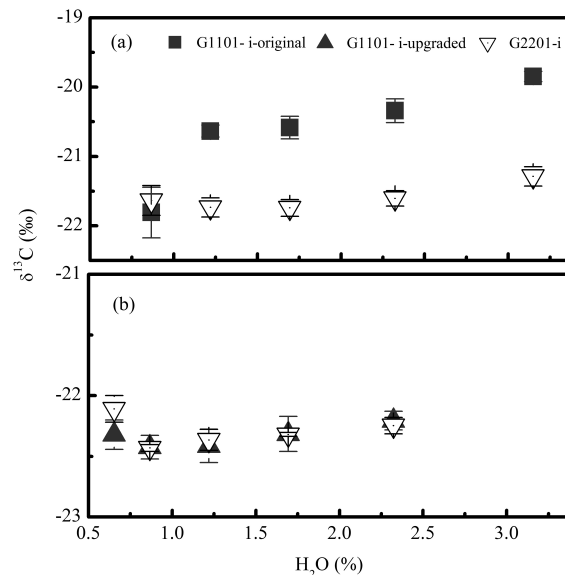


Figure 5. Sensitivity of the measured $\delta^{13}\text{C}$ by G1101-i and G2201-i on water vapor mixing ratio. Panel (a) shows sensitivity measured before G1101-i was upgraded (G1101-i-original and G2201-i) and (b) sensitivity measured after G1101-i was upgraded (G1101-i-upgraded and G2201-i).

nology, however, the residual errors of CO_2 showed substantially large values with increasing water vapor concentration (Nara et al., 2012). The incompatibility of these results indicates the need for more precise experiments to evaluate the transferability of water correction functions (Kwok et al., 2015). Moreover, potential long-term drift of the water vapor correction coefficients of individual instruments needs to be assessed (Nara et al., 2012; Rella et al., 2013).

In this study, the standard deviations of $\delta^{13}\text{C}$ measured by G2201-i (0.07 and 0.08 ‰) under a dew point in the range 5–20 °C are better than the precision given by manufacturer (0.15 ‰), and the standard deviation of $\delta^{13}\text{C}$ measured by G1101-i-upgraded (0.10 ‰) is also smaller than the specified precision. These results indicate that the water corrections embedded in the instruments' software work sufficiently within the dew point range of 5–20 °C.

3.5 Atmospheric measurement

The $\delta^{13}\text{C}$ of atmospheric CO_2 was measured continuously by G1101-i-original and G2201-i analyzers and by G1101-i-upgraded and G2201-i analyzers. The temporal variations of atmospheric $\delta^{13}\text{C}$, the difference between G1101-i and G2201-i analyzers, and the distribution of differences are shown in Fig. 6. The measured atmospheric $\delta^{13}\text{C}$ values were calibrated using Ref1 and Ref3, and Ref2 was used as a quality control gas to assess the accuracy of atmospheric sample measurements (Fig. 7).

Atmospheric $\delta^{13}\text{C}$ measured by G1101-i and G2201-i showed good agreement, and both instruments captured the rapid changes in atmospheric $\delta^{13}\text{C}$ on hourly to diurnal cycle scales. Before G1101-i was upgraded (DOY 164–174), atmospheric $\delta^{13}\text{C}$ measured by G1101-i-original and G2201-i ranged from -13.24 to -7.47 and -13.41 to -7.62 ‰, with average values of -9.49 ± 1.22 and -9.42 ± 1.17 ‰, respectively. The difference between $\delta^{13}\text{C}$ measured by G1101-i-original and G2201-i analyzers ranged from -0.62 to 0.76 ‰, with an average value of 0.07 ± 0.24 ‰. The difference exhibits a Gaussian distribution. A significant systematic bias of $\delta^{13}\text{C}$ values was identified between these two analyzers (t test, $p < 0.01$). After G1101-i was upgraded (DOY 348–356), atmospheric $\delta^{13}\text{C}$ measured by G1101-i-upgraded and G2201-i ranged from -14.08 to -8.64 and -13.89 to -9.06 ‰, with average values of -10.61 and -10.56 ‰, respectively. The difference of $\delta^{13}\text{C}$ measured by G1101-i-upgraded and G2201-i analyzers ranged from -0.57 to 0.85 ‰, with an average value of 0.05 ± 0.30 ‰. A significant systematic bias of $\delta^{13}\text{C}$ values still existed between these two analyzers (t test, $p = 0.018$). In addition, field measured values of Ref2 during the atmospheric measurement period (DOY 164–174 and DOY 348–356) were used to assess the stability and accuracy of both analyzers (Fig. 7). During the first atmospheric measurement period, the average $\delta^{13}\text{C}$ values of Ref2 were -21.32 ± 0.51 and -21.91 ± 0.12 ‰ for G1101-i-original and G2201-i, respectively. After calibration, the average $\delta^{13}\text{C}$ values were -20.30 ± 0.40 and -20.56 ± 0.17 ‰, respectively. The accuracy (the difference between calibration and actual values) respectively ranged from -0.70 to 0.91 and -0.42 to 0.19 ‰, with average values of 0.09 ± 0.40 and -0.17 ± 0.17 ‰. During the second atmospheric measurement period, the average $\delta^{13}\text{C}$ values of Ref2 were -24.37 ± 0.59 and -21.92 ± 0.18 ‰ for G1101-i-upgraded and G2201-i. After

calibration, the average $\delta^{13}\text{C}$ values were -20.56 ± 0.23 and -20.57 ± 0.09 ‰, respectively. The accuracy ranged from -0.60 to 0.30 and -0.42 to 0.02 ‰, with average values of -0.17 ± 0.23 and -0.18 ± 0.09 ‰, respectively. These results indicate that G2201-i is more stable than G1101-i, which is consistent with the Allan variation results.

4 Discussion

4.1 Calibration scheme of IRIS instruments

In general, all of the IRIS instruments aim to maintain high enough precision and accuracy such that the data are traceable to international scales. However, sensitivity to changing environmental conditions (e.g., temperature dependence) and dependence of $\delta^{13}\text{C}$ on the CO_2 concentration affect the performance of IRIS measurements (Wada et al., 2011; Guillon et al., 2012; Wen et al., 2013). Reliable and accurate measurements similar to that of IRMS can be obtained with proper calibration (Bowling et al., 2005; Guillon et al., 2012; Hammer et al., 2013; Vogel et al., 2013; Wen et al., 2013). In theory, both issues of delta scale stretching and the concentration dependence should be corrected by generating multiple delta values over a range of mixing ratios under ambient conditions. In practice, ignoring the effect of the delta scale stretching, the two-point mixing ratio gain and offset calibration method was successfully applied to calibrate the mixing ratios of $^{12}\text{CO}_2$ and $^{13}\text{CO}_2$ separately (Bowling et al., 2003; Wen et al., 2013). For the instrument performance diagnoses, it was suggested that another reference gas be measured to monitor the long-term precision and accuracy. Three-point or higher calibration schemes with CO_2 concentration signals spanning a range of ambient concentrations were suggested to ensure the linearity of the analyzer and diagnose the instrument performance. With proper calibration frequency, the instrument drifts would be eliminated. Calibration frequency and sampling interval are instrument-specific characteristics. Note that considering the $\delta^{13}\text{C}$ dependence on H_2O , researchers should consider drying moist sample air when H_2O is above 2.4 % as is factory-recommended, even though the water correction works sufficiently well (Fig. 5).

4.2 Error propagation through the Keeling analysis

Figure 8 shows the dependence of the $\delta^{13}\text{C}$ difference between G1101-i-original and G2201-i and between G1101-i-upgraded and G2201-i on water vapor concentration and CO_2 mixing ratio. Before and after G1101-i was upgraded, there was no significant correlation between the $\delta^{13}\text{C}$ difference and CO_2 mixing ratio (Fig. 8a and 8b). Before G1101-i was upgraded, a significant linear correlation was observed between the $\delta^{13}\text{C}$ difference and water vapor concentration ($P < 0.01$, Fig. 8c); after the upgrade of G1101-i, there was no significant correlation between the $\delta^{13}\text{C}$ difference and water vapor concentration ($P > 0.05$, Fig. 8d). This re-

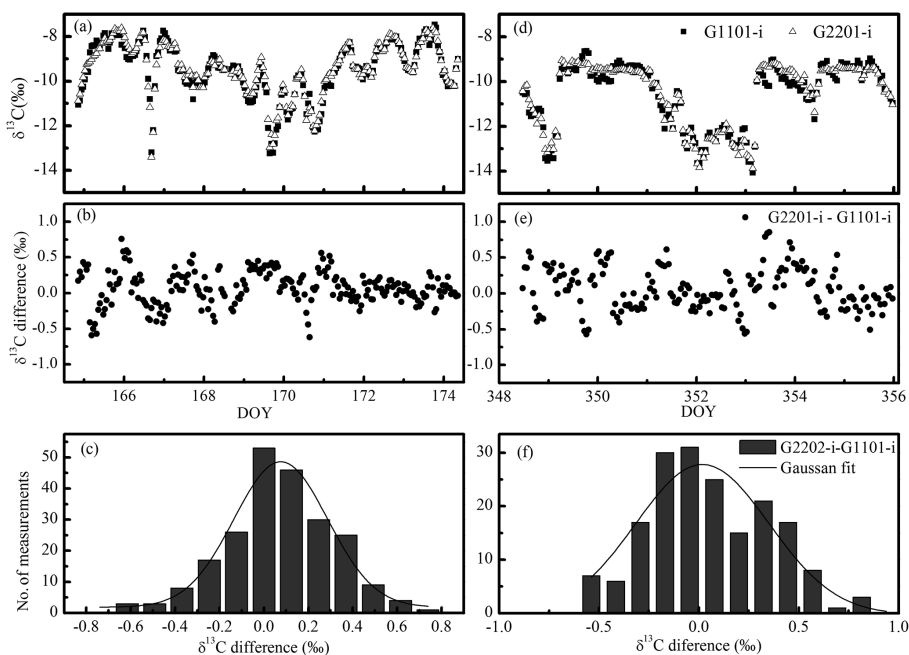


Figure 6. Time variations of (a) and (d) hourly atmospheric $\delta^{13}\text{C}$, (b) and (e) difference between the Picarro G1101-i and G2201-i analyzers, and (c) and (f) histogram of the differences. The left panels (a, b, c) show time variations measured before G1101-i was upgraded (G1101-i-original) (DOY 164–174) and the right panels (d, e, f) show those measured after G1101-i was upgraded (G1101-i-upgraded) (DOY 348–356).

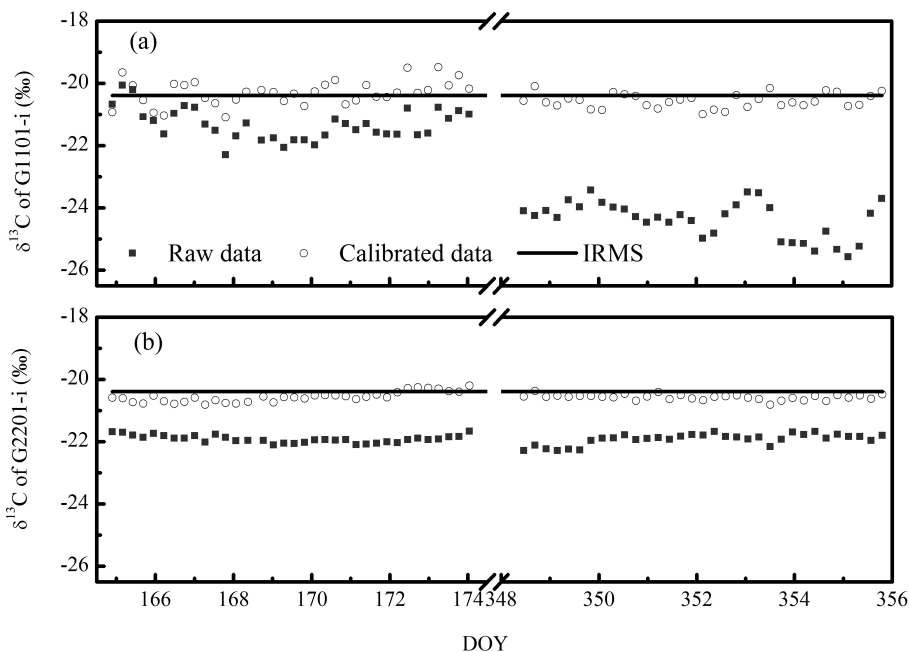


Figure 7. Time series of the 10 min averaged $\delta^{13}\text{C}$ of quality control gas (Ref2) monitored by (a) G1101-i analyzer and (b) G2201-i analyzer.

relationship was mainly due to the upgrade of G1101-i, which excluded $\delta^{13}\text{C}$ measurement errors that originated from variations in water vapor concentration and improved the accuracy of $\delta^{13}\text{C}$ measurement. This result is consistent with the

results of the sensitivity of $\delta^{13}\text{C}$ to water vapor concentration test. In addition, note that the second measurement was conducted in winter when the atmospheric water vapor con-

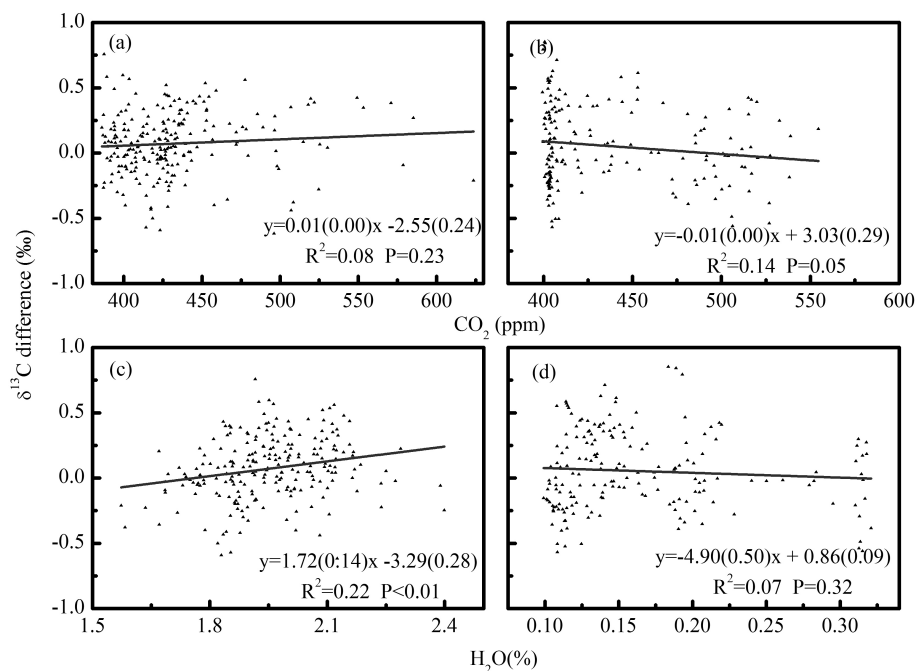


Figure 8. Dependence of the atmospheric $\delta^{13}\text{C}$ difference between the Picarro G1101-i and G2201-i analyzers on the CO_2 and H_2O concentration. Panels (a) and (c) show dependence measured before G1101-i was upgraded (G1101-i-original) (DOY 164–174), and (b) and (d) show dependence measured after G1101-i was upgraded (G1101-i-upgraded) (DOY 348–356).

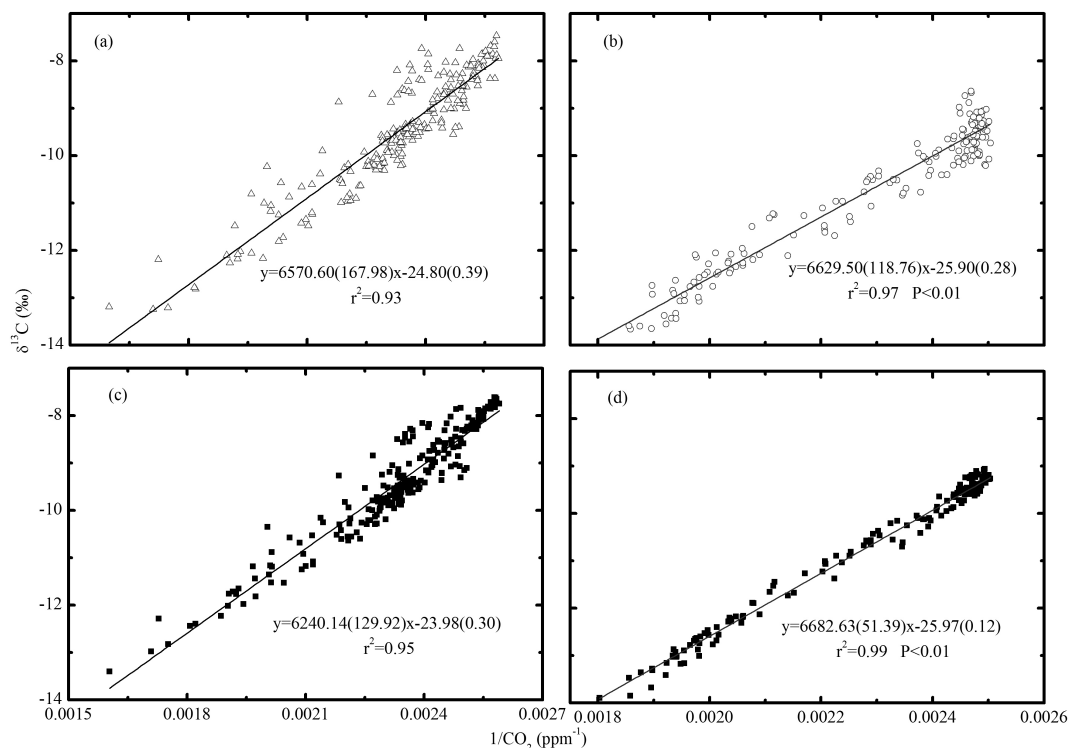


Figure 9. Keeling plot of the calibrated atmospheric $\delta^{13}\text{C}$ against the reciprocal of the calibrated CO_2 concentration for the Picarro (a, b) G1101-i and (c, d) G2201-i analyzers. Panels (a) and (c) show plots measured before G1101-i was upgraded (G1101-i-original) (DOY 164–174), and (b) and (d) show plots measured after G1101-i was upgraded (G1101-i-upgraded) (DOY 348–356). Both daytime and nighttime data were used.

centration was relatively low and the water vapor interference was small.

The isotopic composition of source CO₂ ($\delta^{13}\text{C}_\text{S}$) was used to gain insight into the potential local CO₂ sources and underlying mechanisms at different temporal and spatial scales. In this study, $\delta^{13}\text{C}_\text{S}$ was calculated using the calibration dataset of $\delta^{13}\text{C}$ and 1/CO₂ by the Keeling plot intercept method (Keeling, 1958; Fig. 9). The total CO₂ was calculated using the ¹²CO₂ and ¹³CO₂ from the Picarro data. During the first atmospheric measurement period, the $\delta^{13}\text{C}_\text{S}$ values were -24.80 ± 0.39 and -23.98 ± 0.30 ‰, with a mean difference of 0.82‰, respectively, for G1101-i-original with a range of CO₂ concentrations from 390.92 to 630.92 ppm and G2201-i with a range of CO₂ concentrations from 391.76 to 631.29 ppm. Note that the uncertainties are the standard error of the intercept from the fitting algorithm. If we assumed that the atmospheric $\delta^{13}\text{C}$ is a linear function of 1/CO₂ with a small concentration-dependent error d (Eq. 18; Wen et al., 2013), then error propagation through the concentration dependence would be a function of ε with respect to the intercept of the Keeling plot. When $\varepsilon = 0.05$ ‰, this error would propagate through the Keeling plot and cause a difference of 0.99‰. This result is close to the actual difference of 0.82‰ between G1101-i-original and G2201-i. When we used only the nighttime data (22:00–04:00) for the Keeling analysis, the $\delta^{13}\text{C}_\text{S}$ values were -28.35 ± 1.34 and -27.11 ± 1.02 ‰ for G1101-i-original and G2201-i, respectively, with a mean difference of 1.24‰. The $\delta^{13}\text{C}_\text{S}$ value deduced from nighttime data was a mixed value of various local CO₂ sources, including the combustion of natural gas, gasoline, and coal as well as the respiration of plants and soil (Pang et al., 2016a).

During the second atmospheric measurement period, the $\delta^{13}\text{C}_\text{S}$ values were -25.90 ± 0.28 and -25.97 ± 0.12 ‰, with a mean difference of 0.07‰, for G1101-i-upgraded with a range of CO₂ concentrations from 398.51 to 552.66 ppm and G2201-i with a range of CO₂ concentration from 399.92 to 555.90 ppm, respectively. When we used only the nighttime data (22:00–04:00) for the Keeling analysis, the $\delta^{13}\text{C}_\text{S}$ values were -26.05 ± 0.16 and -25.69 ± 0.41 ‰, with a mean difference of 0.36‰ for G1101-i-upgraded and G2201-i, respectively. The systematic bias of $\delta^{13}\text{C}_\text{S}$ decreased from 1.24‰ between G1101-i-original and G2201-i to 0.36‰ between G1101-i-upgraded and G2201-i. The results confirm that we should pay attention to the measurement difference resulting from the uncorrected dependencies on CO₂ or H₂O concentrations among different IRIS instruments and that this difference will result in error propagation through Keeling plot analysis (Wen et al., 2013).

The potential problems caused by incompatibility include the integrity of an internal calibration scale and modifications to analytical procedures in decade-long records (Levin et al., 2012). In this study, the Keeling plot intercepts of G1101-i and G2201-i measurements should be identical because of the common air samples. Differences in the Keeling plot intercepts of 1.24 or 0.36‰ were caused by a system-

atic error between G1101-i (before and after upgrade) and G2201-i. Note that the uncertainty of the Keeling plot intercept was related to its underlying assumption, CO₂ range, and uncertainty in the CO₂ and isotopic measurements. Generally speaking, the standard error of the Keeling plot intercept should be less than 1‰ (Pataki et al., 2003; Zobitz et al., 2006).

5 Conclusion

In this study, the performance and comparability of Picarro G1101-i and G2201-i CO₂ $\delta^{13}\text{C}$ analyzers was evaluated. The main conclusions are as follows.

1. The Allan variation test indicates that the best precision was 0.08–0.15 and 0.01–0.04‰, measured respectively by G1101-i-original and G2201-i with a CO₂ range from 368.1 to 550.1 ppm; the 5 min precision was 0.24–0.34 and 0.08–0.12‰, respectively. With proper calibration, high enough precision (± 0.1 ‰) for $\delta^{13}\text{C}$ research, similar to that of IRMS, should be obtainable by all of the IRIS instruments. It is difficult, however, to achieve ± 0.01 ‰ precision, as recommended by the Global Atmosphere Watch Programme of the World Meteorological Organization (WMO-GAW; WMO, 2011).
2. For the gradient switching test lasting 48 h among Ref1, Ref2, and Ref3, the dependence of $\delta^{13}\text{C}$ on the CO₂ concentration was 0.46‰ per 100 ppm for G1101-i-original and 0.09‰ per 100 ppm for G2201-i in the range of 368.1–550.1 ppm, and the drift of the instruments ranged from 0.92 to 1.09 and 0.19 to 0.37‰, respectively. After calibration by the two-point mixing ratio gain and offset calibration method, the average $\delta^{13}\text{C}$ values of Ref1, Ref2, and Ref3 were -20.34 ± 0.07 ‰ by G1101-i-original and -20.45 ± 0.09 ‰ by G2201-i, similar to the actual values measured by IRMS (-20.38 ± 0.06 ‰).
3. With dew point temperatures in the range of 5–20 °C, the sensitivity of $\delta^{13}\text{C}$ to the water vapor mixing ratio was 1.01‰/‰ H₂O and 0.09‰/‰ H₂O by G1101-i-original and G2201-i during the first test (before the upgrade of G1101-i) and 0.15‰/‰ H₂O and 0.13‰/‰ H₂O by G1101-i-upgraded and G2201-i during the second test (after the upgrade of G1101-i). The standard deviations of $\delta^{13}\text{C}$ measured by G1101-i-upgraded and G2201-i were ~ 0.10 and ~ 0.08 ‰. These results indicate that the water corrections embedded in the instruments' software work sufficiently within the dew point range of 5–20 °C.
4. Atmospheric $\delta^{13}\text{C}$ measured by G1101-i and G2201-i captured the rapid changes in atmospheric $\delta^{13}\text{C}$ on

hourly to diurnal cycle scales. Before G1101-i was upgraded (DOY 164–174), the difference of hourly $\delta^{13}\text{C}$ averages measured by G1101-i-original and G2201-i analyzers ranged from -0.62 to 0.76‰ , with an average value of $0.07 \pm 0.24\text{‰}$. After G1101-i was upgraded (DOY 348–356), the difference in hourly $\delta^{13}\text{C}$ averages measured by G1101-i-upgraded and G2201-i analyzers ranged from -0.57 to 0.85‰ , with an average value of $0.05 \pm 0.30\text{‰}$. This difference exhibits a Gaussian distribution. Before the upgrade of G1101-i, a significant linear correlation was observed between the $\delta^{13}\text{C}$ difference and water vapor concentration ($P < 0.01$), but there is no significant correlation ($P > 0.05$) after the upgrade of G1101-i. This is mainly due to the improvement of the interference of water vapor in the $\delta^{13}\text{C}$ measurement by the upgraded algorithm of the G1101-i software. The difference of Keeling intercept values between G1101-i and G2201-i decreased from 1.24 to 0.36‰ , which indicates the importance of consistency among different IRIS instruments.

6 Data availability

The dataset for G1101-i and G2201-i analyzers' tests are available for ordering free of charge at https://www.researchgate.net/publication/301644542_Inter-comparison_of_two_cavity_ring-down_spectroscopy_analyzers_for_atmospheric_13CO2_12CO2_measurement (Pang et al., 2016b).

Acknowledgements. This study was supported by the National Natural Science Foundation of China (41571130043, 31290221, and 31470500) and the National Key Research and Development Program of China (2016YFC0500102).

Edited by: T. F. Hanisco

Reviewed by: L. R. Welp and one anonymous referee

References

- Allan, D. W.: Should the classical variance be used as a basic measure in standards metrology?, *IEEE T. Instrum. Meas.*, 1001, 646–654, 1987.
- Bowling, D. R., Sargent, S. D., Tanner, B. D., and Ehleringer, J. R.: Tunable diode laser absorption spectroscopy for stable isotope studies of ecosystem-atmosphere CO_2 exchange, *Agr. Forest Meteorol.*, 118, 1–19, doi:10.1016/s0168-1923(03)00074-1, 2003.
- Bowling, D. R., Burns, S. P., Conway, T. J., Monson, R. K., and White, J. W. C.: Extensive observations of CO_2 carbon isotope content in and above a high-elevation subalpine forest, *Global Biogeochem. Cy.*, 19, GB3023, doi:10.1029/2004gb002394, 2005.
- Chen, H., Winderlich, J., Gerbig, C., Hofer, A., Rella, C. W., Crosson, E. R., Van Pelt, A. D., Steinbach, J., Kolle, O., Beck, V., Daube, B. C., Gottlieb, E. W., Chow, V. Y., Santoni, G. W., and Wofsy, S. C.: High-accuracy continuous airborne measurements of greenhouse gases (CO_2 and CH_4) using the cavity ring-down spectroscopy (CRDS) technique, *Atmos. Meas. Tech.*, 3, 375–386, doi:10.5194/amt-3-375-2010, 2010.
- Flowers, B. A., Powers, H. H., Dubey, M. K., and McDowell, N. G.: Inter-comparison of two high-accuracy fast-response spectroscopic sensors of carbon dioxide: a case study, *Atmos. Meas. Tech.*, 5, 991–997, doi:10.5194/amt-5-991-2012, 2012.
- Friedrichs, G., Bock, J., Temps, F., Fietzek, P., Kortzinger, A., and Wallace, D. W. R.: Toward continuous monitoring of seawater $^{13}\text{CO}_2/^{12}\text{CO}_2$ isotope ratio and pCO_2 : Performance of cavity ringdown spectroscopy and gas matrix effects, *Limnol. Oceanogr.-Meth.*, 8, 539–551, doi:10.4319/lom.2010.8.539, 2010.
- Griffis, T. J.: Tracing the flow of carbon dioxide and water vapor between the biosphere and atmosphere: A review of optical isotope techniques and their application, *Agr. Forest Meteorol.*, 174, 85–109, doi:10.1016/j.agrformet.2013.02.009, 2013.
- Griffis, T. J., Baker, J. M., Sargent, S. D., Tanner, B. D., and Zhang, J.: Measuring field-scale isotopic CO_2 fluxes with tunable diode laser absorption spectroscopy and micrometeorological techniques, *Agr. Forest Meteorol.*, 124, 15–29, doi:10.1016/j.agrformet.2004.01.009, 2004.
- Griffith, D. W. T., Deutscher, N. M., Caldow, C., Kettlewell, G., Riggensbach, M., and Hammer, S.: A Fourier transform infrared trace gas and isotope analyser for atmospheric applications, *Atmos. Meas. Tech.*, 5, 2481–2498, doi:10.5194/amt-5-2481-2012, 2012.
- Guillon, S., Pili, E., and Agrinier, P.: Using a laser-based CO_2 carbon isotope analyser to investigate gas transfer in geological media, *Applied Physics B-Lasers and Optics*, 107, 449–457, doi:10.1007/s00340-012-4942-8, 2012.
- Hammer, S., Griffith, D. W. T., Konrad, G., Vardag, S., Caldow, C., and Levin, I.: Assessment of a multi-species in situ FTIR for precise atmospheric greenhouse gas observations, *Atmos. Meas. Tech.*, 6, 1153–1170, doi:10.5194/amt-6-1153-2013, 2013.
- Keeling, C. D.: The concentration and isotopic abundances of atmospheric carbon dioxide in rural areas, *Geochim. Cosmochim. Ac.*, 13, 322–334, 1958.
- Kwok, Y. C., Laurent, O., Guemri, A., Philippon, C., Wastine, B., Rella, C. W., Vuillemin, C., Truong, F., Delmotte, M., Kazan, V., Darding, M., Lebègue, B., Kaiser, C., Xueref-Rémy, I., and Ramonet, M.: Comprehensive laboratory and field testing of cavity ring-down spectroscopy analyzers measuring H_2O , CO_2 , CH_4 and CO , *Atmos. Meas. Tech.*, 8, 3867–3892, doi:10.5194/amt-8-3867-2015, 2015.
- Levin, I., C. Veidt, B. Vaughn, G. Brailsford, T. Bromley, R. Heinz, D. Lowe, J. Miller, C. Poß and J. White: No inter-hemispheric $\delta^{13}\text{CH}_4$ trend observed, *Nature*, 486, E3–E4, 2012.
- McManus, J. B., Nelson, D. D., Shorter, J. H., Jimenez, R., Herson, S., Saleska, S., and Zahniser, M.: A high precision pulsed quantum cascade laser spectrometer for measurements of stable isotopes of carbon dioxide, *J. Mod. Optic.*, 52, 2309–2321, doi:10.1080/09500340500303710, 2005.
- Mohn, J., Werner, R. A., Buchmann, B., and Emmenegger, L.: High-precision $\delta^{13}\text{CO}_2$ analysis by FTIR spectroscopy us-

- ing a novel calibration strategy, *J. Mol. Struct.*, 834, 95–101, doi:10.1016/j.molstruc.2006.09.024, 2007.
- Mohn, J., Zeeman, M. J., Werner, R. A., Eugster, W., and Emmenegger, L.: Continuous field measurements of $\delta^{13}\text{C}\text{O}_2$ and trace gases by FTIR spectroscopy, *Isotopes Environ. Health Stud.*, 44, 241–251, doi:10.1080/10256010802309731, 2008.
- Nara, H., Tanimoto, H., Tohjima, Y., Mukai, H., Nojiri, Y., Katsumata, K., and Rella, C. W.: Effect of air composition (N_2 , O_2 , Ar, and H_2O) on CO_2 and CH_4 measurement by wavelength-scanned cavity ring-down spectroscopy: calibration and measurement strategy, *Atmos. Meas. Tech.*, 5, 2689–2701, doi:10.5194/amt-5-2689-2012, 2012.
- Pang, J., Wen, X., and Sun, X.: Mixing ratio and carbon isotopic composition investigation of atmospheric CO_2 in Beijing, China, *Sci. Total Environ.*, 539, 322–330, 2016a.
- Pang, J., Wen, X., Sun, X., and Huang, K.: Inter-comparison of two cavity ring-down spectroscopy analyzers for atmospheric $^{13}\text{CO}_2/^{12}\text{CO}_2$ measurement, available at: https://www.researchgate.net/publication/301644542_Inter-comparison_of_two_cavity_ring-down_spectroscopy_analyzers_for_atmospheric_13CO2_12CO2_measurement, 2016b.
- Pataki, D. E., Bowling, D. R., Ehleringer, J. R., and Zobitz, J. M.: High resolution atmospheric monitoring of urban carbon dioxide sources, *Geophys. Res. Lett.*, 33, L03813, doi:10.1029/2005gl024822, 2006.
- Rella, C. W., Chen, H., Andrews, A. E., Filges, A., Gerbig, C., Hatakka, J., Karion, A., Miles, N. L., Richardson, S. J., Steinbacher, M., Sweeney, C., Wastine, B., and Zellweger, C.: High accuracy measurements of dry mole fractions of carbon dioxide and methane in humid air, *Atmos. Meas. Tech.*, 6, 837–860, doi:10.5194/amt-6-837-2013, 2013.
- Schaeffer, S. M., Miller, J. B., Vaughn, B. H., White, J. W. C., and Bowling, D. R.: Long-term field performance of a tunable diode laser absorption spectrometer for analysis of carbon isotopes of CO_2 in forest air, *Atmos. Chem. Phys.*, 8, 5263–5277, doi:10.5194/acp-8-5263-2008, 2008.
- Sturm, P., Eugster, W., and Knohl, A.: Eddy covariance measurements of CO_2 isotopologues with a quantum cascade laser absorption spectrometer, *Agr. Forest Meteorol.*, 152, 73–82, doi:10.1016/j.agrformet.2011.09.007, 2012.
- Tuzson, B., Zeeman, M. J., Zahniser, M. S., and Emmenegger, L.: Quantum cascade laser based spectrometer for in situ stable carbon dioxide isotope measurements, *Infrared Phys. Techn.*, 51, 198–206, doi:10.1016/j.infrared.2007.05.006, 2008.
- Vogel, F. R., Huang, L., Ernst, D., Giroux, L., Racki, S., and Worthy, D. E. J.: Evaluation of a cavity ring-down spectrometer for in situ observations of $^{13}\text{CO}_2$, *Atmos. Meas. Tech.*, 6, 301–308, doi:10.5194/amt-6-301-2013, 2013.
- Wada, R., Pearce, J. K., Nakayama, T., Matsumi, Y., Hiyama, T., Inoue, G., and Shibata, T.: Observation of carbon and oxygen isotopic compositions of CO_2 at an urban site in Nagoya using Mid-IR laser absorption spectroscopy, *Atmos. Environ.*, 45, 1168–1174, 2011.
- Wahl, E. H., Fidric, B., Rella, C. W., Koulikov, S., Kharlamov, B., Tan, S., Kachanov, A. A., Richman, B. A., Crosson, E. R., Paldus, B. A., Kalaskar, S., and Bowling, D. R.: Applications of cavity ring-down spectroscopy to high precision isotope ratio measurement of $^{13}\text{C}/^{12}\text{C}$ in carbon dioxide, *Isotopes Environ. Health Stud.*, 42, 21–35, doi:10.1080/10256010500502934, 2006.
- Wehr, R., Kassi, S., Romanini, D., and Gianfrani, L.: Optical feedback cavity-enhanced absorption spectroscopy for in situ measurements of the ratio $^{13}\text{C}:^{12}\text{C}$ in CO_2 , *Appl. Phys. B-Lasers O.*, 92, 459–465, 2008.
- Wen, X. F., Sun, X. M., Zhang, S. C., Yu, G. R., Sargent, S. D., and Lee, X.: Continuous measurement of water vapor D/H and $^{18}\text{O}/^{16}\text{O}$ isotope ratios in the atmosphere, *J. Hydrol.*, 349, 489–500, doi:10.1016/j.jhydrol.2007.11.021, 2008.
- Wen, X. F., Zhang, S. C., Sun, X. M., Yu, G. R., and Lee, X.: Water vapor and precipitation isotope ratios in Beijing, China, *J. Geophys. Res.-Atoms.*, 115, D01103, doi:10.1029/2009jd012408, 2010.
- Wen, X. F., Lee, X., Sun, X. M., Wang, J. L., Tang, Y. K., Li, S. G., and Yu, G. R.: Inter-comparison of four commercial analyzers for water vapor isotope measurement, *J. Atmos. Ocean. Tech.*, 29, 235–247, 2012.
- Wen, X.-F., Meng, Y., Zhang, X.-Y., Sun, X.-M., and Lee, X.: Evaluating calibration strategies for isotope ratio infrared spectroscopy for atmospheric $^{13}\text{CO}_2/^{12}\text{CO}_2$ measurement, *Atmos. Meas. Tech.*, 6, 1491–1501, doi:10.5194/amt-6-1491-2013, 2013.
- Werle, P., Mucke, R., and Slemr, F.: The limits of signal averaging in atmospheric trace-gas monitoring by tunable diode-laser absorption-spectroscopy (TDLAS), *Appl. Phys. B-Photo.*, 57, 131–139, doi:10.1007/bf00425997, 1993.
- Werner, C., Schnyder, H., Cuntz, M., Keitel, C., Zeeman, M. J., Dawson, T. E., Badeck, F.-W., Brugnoli, E., Ghashghaie, J., Grams, T. E. E., Kayler, Z. E., Lakatos, M., Lee, X., Máguas, C., Ogée, J., Rascher, K. G., Siegwolf, R. T. W., Unger, S., Welker, J., Wingate, L., and Gessler, A.: Progress and challenges in using stable isotopes to trace plant carbon and water relations across scales, *Biogeosciences*, 9, 3083–3111, doi:10.5194/bg-9-3083-2012, 2012.
- Wingate, L., Ogee, J., Burrell, R., Bosc, A., Devaux, M., Grace, J., Loustau, D., and Gessler, A.: Photosynthetic carbon isotope discrimination and its relationship to the carbon isotope signals of stem, soil and ecosystem respiration, *New Phytol.*, 188, 576–589, doi:10.1111/j.1469-8137.2010.03384.x, 2010.
- WMO: Report no. 194. 15th WMO/IAEA Meeting of Experts on Carbon Dioxide, Other Greenhouse Gases and Related Tracers Measurement Techniques, Geneva WMO/TD-No. 1553, 2011.
- Yakir, D., and Sternberg, L. D. L.: The use of stable isotopes to study ecosystem gas exchange, *Oecologia*, 123, 297–311, doi:10.1007/s004420051016, 2000.
- Zobitz, J. M., Keener, J. P., Schnyder, H., and Bowling, D. R.: Sensitivity analysis and quantification of uncertainty for isotopic mixing relationships in carbon cycle research, *Agr. Forest Meteorol.*, 136, 56–75, 2006.